communications earth & environment

Article

A Nature Portfolio journal

https://doi.org/10.1038/s43247-026-03770-y

Dual clumped isotopes in foraminiferal calcite reveal kinetic bias in some species

Amelia Jane Davies[1,2] ✉, Marion Peral[3], Jonathan Erez[4], Adam Levi[4], David Evans[5], Oliver Friedrich[6], Thibaut Caley[3], Romi Nambiar[1,5], Douglas Coenen[1], Philip Tauxe Staudigel[1], Mattia Tagliavento[1,7], Miguel Bernecker[1] & Jens Fiebig[1] ✉

Clumped isotope (Δ_{47}) analyses of foraminifera provide a powerful means to reconstruct upper and bottom water temperatures, independent of seawater $\delta^{18}O$ and elemental composition. We show statistically significant disequilibrium in the dual (Δ_{47}-Δ_{48}) clumped isotope composition of some large benthic foraminifera, while other large benthic foraminifera plot within analytical uncertainty of Δ_{47}–Δ_{48} equilibrium. This deviation suggests the influence of reaction kinetics, such as kinetic effects during CO_2 absorption or a combination of ion attachment/detachment effects at the solution-crystal interface and slight DIC disequilibrium. Measured core-top, planktic and deep-sea benthic foraminifera plot within the 95% confidence level of empirical Δ_{47}-Δ_{48} equilibrium, although additional measurements are required to confidently exclude kinetic Δ_{47}-Δ_{48} bias. Dual clumped isotope measurements of large benthic foraminifera from the Eocene of the Paris and Hampshire basins that conform with Δ_{47}-Δ_{48} equilibrium (95% confidence level) further support existing evidence for surface ocean temperatures ~12–17 °C warmer than today.

The reconstruction of ocean water temperature and the oxygen isotope composition of seawater ($\delta^{18}O_{sw}$) is key to understanding past climate change and ocean dynamics. Foraminiferal $\delta^{18}O$ values have been used to reconstruct seawater temperature evolution as far back as the Cretaceous, exploiting the global abundance of foraminifera in abyssal, intermediate and surface water masses[1–6]. Calcifying foraminifera may be split into two groups, the imperforate or porcelaneous foraminifera and the perforate or calcitic radial, otherwise known as hyaline, foraminifera. Hyaline foraminiferal tests range from small simple forms with only a few chambers, typical of planktic and small benthic foraminifera, to highly complex, multi-chambered tests, as observed in large benthic foraminifera (LBF). Planktic and small benthic foraminifera produce shells of low-Mg calcite, and planktic foraminifera may host photosynthetic symbionts[7]. Epifaunal LBF are an informal polyphyletic group of extant and fossil taxa with a long[7–10] fossil record from the Carboniferous to present[8]. Their grouping is based on ecological and morphological characteristics that evolved multiple times from several unrelated benthic clades, key amongst which are their large test sizes and complex internal morphologies[9]. They inhabit depths within the photic zone and are often adapted to host algal and diatom photo symbionts[11]. Whilst LBF differ morphologically and ecologically from core-top planktic and benthic foraminifera it is not clear whether a general model of biomineralization applies to all hyaline foraminifera[10,12].

Despite its widespread application, the accurate reconstruction of seawater temperature from foraminiferal $\delta^{18}O$ is constrained by several uncertainties. Paleotemperature reconstruction by oxygen isotope thermometry of foraminifera requires a-priori knowledge or assumption of $\delta^{18}O_{sw}$, which can vary both geographically and through time. An understanding of ecological factors surrounding foraminiferal growth which impact foraminiferal $\delta^{18}O$, such as growth seasonality and depth of calcification, is also imperative. Furthermore, $\delta^{18}O$ temperature estimates may be biased by biologically mediated disequilibrium effects, which have been linked to either the carbonate ion concentration [CO_3^{2-}] or pH of seawater surrounding foraminiferal tests and photosynthesis in symbiont bearing species[11,13–17]. Biologically mediated disequilibrium in the oxygen isotope composition of foraminiferal calcite has led to the development and use of both field collected and laboratory cultured species-specific calibrations[17–22].

More recently, the clumped (Δ_{47}) isotope thermometer has been applied to foraminifera[23–29]. In thermodynamic equilibrium, the clumping of ^{13}C-^{18}O in marine carbonates is independent of seawater-$\delta^{18}O$, as ^{13}C-^{18}O clumping follows a self-reaction of isotope exchange

[1]Institut für Geowissenschaften, Goethe Universität Frankfurt, Frankfurt am Main, Germany. [2]Institut für Geologie und Mineralogie, Universität zu Köln, Köln, Germany. [3]Université de Bordeaux, CNRS, Bordeaux INP, EPOC, UMR, Pessac, France. [4]Institute of Earth Sciences, The Hebrew University of Jerusalem, Jerusalem, Israel. [5]School of Ocean and Earth Science, University of Southampton, Southampton, UK. [6]Institute of Earth Sciences, Heidelberg University, Heidelberg, Germany. [7]Division of Geological and Planetary Sciences, California Institute of Technology, Pasadena, CA, USA. ✉e-mail: adavies@uni-koeln.de; jens.fiebig@em.uni-frankfurt.de

$M^{13}C^{16}O_3 + M^{12}C^{18}O^{16}O_2 \rightleftharpoons M^{13}C^{18}O^{16}O_2 + M^{12}C^{16}O_3$ (where M is a metal such as Ca)[30]. Carbonate clumped isotope thermometry therefore offers a distinct advantage over oxygen isotope and trace element ratio thermometry (e.g. Mg/Ca), in that reconstructed temperatures are independent of the elemental and oxygen isotope composition of seawater.

Initial studies of the clumped isotope composition of planktic and small benthic foraminiferal calcite established a single Δ_{47}-temperature relationship that was indistinguishable from the experimentally derived Δ_{47}-temperature relationship of inorganic carbonate[31,32], leading to the first application of the clumped isotope thermometer to fossil foraminiferal archives[33]. Developments in sample preparation and IRMS such as long integration dual inlet (LIDI) methods, have since decreased the sample size requirement for clumped isotope analysis[24,34,35], which, alongside community wide carbonate-based standardization[36], have unlocked foraminiferal archives for clumped isotope measurement. Reported sample size for LIDI methods ranges around 70–200 µg per replicate, requiring 25–40 replicates per sample totalling ~1.5–3 mg calcite[24,34,37,38].

Grouped data from recent calibration studies based on core-top planktic and benthic samples[35,39,40], reprocessed to fit the InterCarb-Carbon Dioxide Equilibrium Scale (ICDES)[41], yield a regression statistically indistinguishable from that of inorganic carbonates. Therefore, both inorganic and foraminiferal datasets have been incorporated into unified Δ_{47}-temperature calibrations[42,43]. Foraminiferal Δ_{47} appears unaffected by pH and salinity at typical marine salinities and ocean pH values[31,35,44]. A recent recompilation[45] of foraminiferal isotope data, however, suggests inconsistencies between Δ_{47}-temperature calibrations of planktic[35,39] and benthic foraminifera[46]. Foraminiferal Δ_{47}-temperature calibrations remain hampered by uncertainties in calcification temperature, largely arising from ambiguities in species-specific calcification depths and seasonality. In particular, planktic foraminifera may experience strong growth temperature variations on changing depth habitat and growth seasonality. Estimated calcification temperatures based on World Ocean Atlas (WOA) at inferred growth depths differ substantially from those derived from measured foraminiferal $\delta^{18}O_{carbonate}$ and best estimated $\delta^{18}O_{seawater}$[39,47]. Consequently, uncertainty persists regarding the extent to which planktic and deep-sea benthic foraminifera precipitate calcite in clumped isotope equilibrium.

Few studies have utilized the Δ_{47} of epifaunal LBF. Prior to recent inter-laboratory calibration efforts, Evans et al[28]. defined a group-specific Δ_{47} temperature calibration relative to the equilibrium calibration made in the same lab[48]. LBF are a promising yet under-utilized archive for reconstructing shallow water temperatures within the photic zone, particularly tropical temperatures during greenhouse climate states, where proxy constraints remain limited[28,49–51]. However, as with low-Mg planktic and deep-sea benthic foraminifera, it remains unclear whether LBF, particularly high-Mg calcite species, biomineralize in clumped isotope equilibrium.

Dual clumped isotope thermometry involves the simultaneous measurement of Δ_{47} and Δ_{48} in CO_2 evolved from the acid digestion of carbonate minerals[52,53]. A significant advantage of dual clumped isotope thermometry over Δ_{47}-only measurements is the ability to identify isotopic disequilibrium in carbonate materials, even when growth temperatures are unknown[53–56]. Dual clumped isotope thermometry, therefore, offers an effective way of identifying disequilibrium isotope effects in foraminiferal carbonate without a priori estimation of depth environment or growth seasonality. Application of the dual clumped isotope thermometer to foraminiferal archives provides an opportunity to re-evaluate and assess the influence of temperature-independent processes on foraminiferal clumped isotope composition. Dual clumped isotope measurement is technically challenging and requires much larger sample sizes than Δ_{47} measurement. However, Δ_{47} precision is higher during dual-inlet Δ_{47}-Δ_{48} measurement, achieving long term standard deviations of Δ_{47} of 0.007-0.009 ‰[53,54].

In this study, we present the dual clumped isotope compositions of hyaline calcitic foraminifera, including tropical field-collected and cultured LBF of species *Operculina ammonoides* and *Amphistegina lobifera*. We demonstrate that some LBF precipitate calcite in clumped isotope disequilibrium while others form calcite at or close to clumped isotope equilibrium. Furthermore, we show that dual clumped isotope thermometry can be used to identify disequilibrium in the clumped isotope composition of LBF when their growth temperatures are unknown. Using this finding, we present Δ_{47} derived temperatures from Eocene LBF of the Hampshire and Paris basins which exhibit Δ_{47}-Δ_{48} values that are consistent with equilibrium. We also examine the Δ_{47}-Δ_{48} values of hyaline calcitic core-top foraminiferal samples of the planktic foraminiferal species *Neogloboquadrina pachyderma* and *Globigerinoides ruber* and the deep-ocean benthic foraminiferal species *Lobatula wuellerstorfi*. The dual clumped isotope compositions of these low-Mg foraminifera plot indistinguishable from empirical Δ_{47}-Δ_{48} equilibrium at the 95% confidence level (CI).

Results

Dual clumped (Δ47 and Δ48) isotope measurements of foraminiferal samples in comparison with empirical equilibrium

The dual clumped isotope (Δ_{47} and Δ_{48}) values of all measured samples are plotted alongside the empirical equilibrium calibration of Fiebig et al[55]. in Fig. 1. In this calibration the theoretical Δ_{47}-temperature relationship[56] is anchored at Earth surface temperatures to the inorganic cave calcites of Devils Hole and Laghetto Basso, which, due to their uniquely slow growth rates, precipitated closest to oxygen and clumped isotope equilibrium[57]. Measured clumped (Δ_{47} and Δ_{48}), $\delta^{18}O$ and $\delta^{13}C$ isotope values of foraminifera are presented in Supplementary Table 1. Unless otherwise specified, clumped isotope temperatures are reported using the calibration of Fiebig et al.[55]. Errors in measured Δ_{47} and Δ_{48} are reported at both the 68% CI (1 standard error) and 95% CI (2 standard errors), calculated in D47crunch[58] and incorporate full propagation of analytical uncertainties, including standardization errors. For cultured foraminifera the isotope composition of the whole sample is reported i.e. Δ_{47}-Δ_{48} of CO_2 from acid digestion of mixed original calcite and calcite growth at culture temperature. Dual clumped isotope values of Eocene fossil LBF are also shown in Fig. 1 and clumped isotope derived growth temperatures from fossil foraminifera given in Supplementary Table 2.

Mean Δ_{47} and Δ_{48} values of all measured foraminifera, except for large benthic foraminifera *A. lobifera*, plot with depletion in Δ_{48} in comparison with the empirical equilibrium calibration line of Fiebig et al.[55]. However, only two samples display Δ_{47}-Δ_{48} values that are distinguishable from equilibrium[55] at the 95% confidence interval (Fig. 1). Both samples correspond to LBF of species *O. ammonoides;* a field-collected sample of LBF *O. ammonoides* from the Great Barrier Reef (SS07613) and cultured sample of *O. ammonoides* (SR50_2LBF). We examine the pattern of dual clumped isotope offsets in grouped modern LBF from empirical equilibrium[55]. To identify disequilibrium in Δ_{48} we assess the difference between measured and expected equilibrium Δ_{48} values[55], where expected equilibrium Δ_{48} is calculated from Δ_{47}-derived temperatures, compared to samples of the inorganic calibration[55]. Using a Welch's T-test the LBF group show a statistically significant Δ_{48} offset ($M = -0.016$, SD 0.015) from inorganic samples of the empirical equilibrium calibration[58] ($t(11.03) = -2.24$, $p = 0.046$).

Measured core-top foraminiferal samples plot within error (95% CI) of dual clumped isotope equilibrium[55] (Fig. 1). However, 3 of 4 core top samples, including *G. ruber* from the Agulhas Current source region, *N. pachyderma* and benthic *L. wuellerstorfi* have Δ_{47}-Δ_{48} values that do not conform with equilibrium at 68% CI[55], exhibiting depletion in Δ_{48}. As described above, we assess the difference between measured and expected equilibrium Δ_{48} values[55], where expected equilibrium Δ_{48} is calculated from Δ_{47}-derived temperatures. When core-top planktic and benthic samples are grouped together, they show a statistically significant offset in Δ_{48} ($M = -0.017$, SD 0.007) from inorganic samples of the empirical equilibrium calibration[55] ($t(6.08) = -3.79$, $p = 0.009$). However, the offset observed in planktic foraminifera alone ($M = -0.016$, 0.008) is not statistically significant ($t(3.03) = -2.86$, $p = 0.071$).

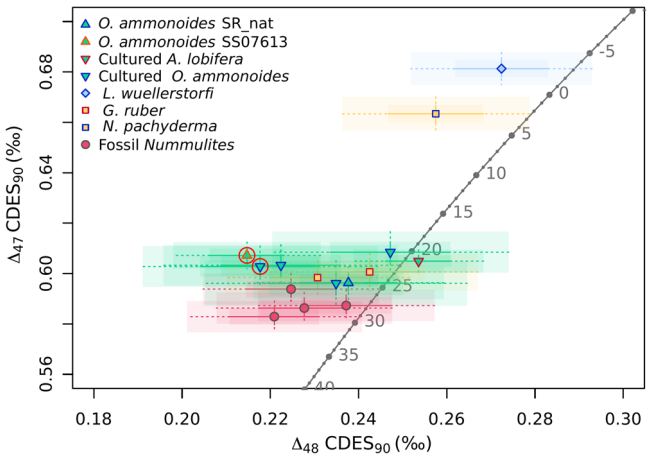

Fig. 1 | Dual clumped isotopic composition of modern and fossil foraminifera compared to the abiogenic empirical equilibrium calibration. The grey line marks the Δ_{47}-Δ_{48}equilibrium calibration of Fiebig et al.[55]. Errors are presented at the 68% (solid error bars) and 95% (dashed error bars) confidence levels. Samples circled in red plot distinguishable from Δ_{47}-Δ_{48} equilibrium at the 95% Cl.

Foraminiferal $\delta^{18}O$, Δ_{47} and Δ_{48} relative to calcification temperature estimates: extent of isotopic disequilibrium in foraminiferal samples

The extent and significance of kinetic isotope effects that might be effective during foraminiferal calcification is best examined in disequilibrium plots where expected Δ_{47}-Δ_{48} values, calculated from measured or assumed calcification temperatures[59], are compared with measured isotopic values (Fig. 2a). This enables identification of samples that are in dual clumped isotope disequilibrium but, by chance, plot within error of the equilibrium Δ_{47}-Δ_{48} relationship shown in Fig. 1, such as observed for brachiopods[60] and coccolithophores[61]. For cultured samples, disequilibrium was calculated as Δ_{47}-Δ_{48} offsets of mixed calcite in comparison with accepted growth temperatures calculated using Eq. 1; this value is fully error propagated to include uncertainty on growth temperatures and fraction of calcite grown under culture conditions (Supplementary Table 3). For all samples, uncertainties in growth temperature (see Supplementary Tables 3 and 4), and the dual clumped isotope temperature relationship[55] are propagated onto analytical uncertainties to allow identification of apparent disequilibrium samples in Fig. 1 whose measured isotopic composition becomes consistent with expected equilibrium values if all uncertainties were considered.

Consideration of independently constrained growth temperatures and associated uncertainties largely confirms the (dis)equilibrium patterns shown by Fig. 1. In this analysis, three of seven LBF samples show significant disequilibrium offsets in either Δ_{47}, or Δ_{48}. *O. ammonoides* collected from the Great Barrier Reef (SS07613) has significant enrichment of 0.013 ± 0.008 ‰ in Δ_{47} and depletion in Δ_{48} of -0.031 ± 0.019 ‰ (Fig. 2a). Cultured *O. ammonoides*, sample SR50_2LBF exhibits significant depletion in Δ_{48} of -0.030 ± 0.028 ‰ and cultured *O. ammonoides*, sample SR50_4LBF, plots with a significant enrichment in Δ_{47} of 0.013 ± 0.011 ‰, at the 95% Cl (Fig. 2a).. Both samples have a measured dual clumped isotope composition that is distinguishable from the Δ_{47}-Δ_{48} empirical equilibrium relationship[55] at the 95% Cl (Fig. 1). *A. lobifera* and field-collected LBF *O. ammonoides* from the Gulf of Eilat (SR_nat), which is the starting material for cultured samples, exhibit no significant disequilibrium in Δ_{47} or Δ_{48} (Fig. 2a), as do cultured samples SR50_1LBF and SR50_3LBF. The (differential) driver of disequilibrium in *O. ammonoides* grown at different temperatures is explored in detail below.

The data shown in Fig. 2a confirm the absence of significant disequilibrium bias in most core-top foraminiferal samples. Three out of four samples plot indistinguishable from the origin (and, hence, from equilibrium) at the 95% Cl if WOA + FAME assumed growth temperature estimates are considered to calculate Δ_{47} and Δ_{48} disequilibrium offsets (Fig. 2a). The only exception to this is *N. pachyderma*. Although its Δ_{47} value still corresponds to the inferred growth temperature at the 95% Cl level, its Δ_{48} value seems to be slightly depleted with respect to the predicted equilibrium value.

All samples exhibit $\delta^{18}O$ depletions relative to expected equilibrium, based on slow-growing mammillary calcites thought to precipitate closest to isotopic equilibrium[57,62,63] (Fig. 2b). Instead, they exhibit oxygen isotope fractionation-temperature relationships more closely aligned with that characteristic of more rapidly precipitated synthetic carbonate[64,65].

Discussion

Disequilibrium in the dual clumped isotope composition of LBF

Three of six measured samples of *O. ammonoides* plot with statistically distinguishable disequilibrium offsets in dual clumped isotope composition in comparison with inferred growth temperatures (Fig. 2a). These observations demonstrate that LBF are prone to subtle disequilibrium bias in their clumped isotope compositions. This conclusion agrees with the findings of Evans et al.[28] who identified disequilibrium in the Δ_{47} temperature relationship of LBF in comparison with inorganic carbonates[48]. However, LBF do not show well correlated patterns of disequilibrium offsets in Δ_{47} and Δ_{48}, i.e. they do not fall along a well-defined Δ_{47} and Δ_{48} trajectory that can be characterized by a specific disequilibrium process (Fig. 2a). All measured LBF exhibit enrichment in $\Delta_{47,}$ relative to mean inferred growth temperatures, underestimating the latter by up to 4.6 ± 3.1 °C when equilibrium Δ_{47}-temperature calibrations are applied[55] (Fig. 3, Supplementary Tables 3 and 4). In addition, grouped data on all LBF show a statistically significant Δ_{48} offset ($M = -0.016$, SD 0.015). However, while some LBF exhibit disequilibrium in Δ_{47} and/or Δ_{48} in comparison with inferred growth temperatures, the dual clumped isotope compositions of three measured *O. ammonoides* samples are consistent with dual clumped isotope equilibrium at inferred growth temperature (Figs. 2, 3). *O. ammonoides* samples SR_nat, SR50-1 and SR50_3 plot within error of Δ_{47}-Δ_{48} equilibrium (Fig. 1) and yield Δ_{47} temperatures within 0.4 °C to 1.6 °C of inferred growth temperature.

Dual clumped isotope disequilibrium is observed in both wild-collected and cultured LBF (Fig. 2a). For cultured samples, the method of calculating the fraction of cultured calcite has no significant impact on calculated Δ_{47}-Δ_{48} disequilibrium values (Supplementary Fig. 1). There is no clear correlation between inferred growth temperature or culture temperature and dual clumped isotope disequilibrium. Furthermore, the range of Δ_{47} and Δ_{48} offsets from equilibrium observed in cultured samples is also observed in field-collected samples (Fig. 2a).

Driving mechanism of isotopic disequilibrium in LBFs

When Δ_{47} and Δ_{48} disequilibrium is calculated relative to WOA derived or measured growth temperatures[59], LBF predominantly plot in the region of Δ_{48} depletion and Δ_{47} enrichment in comparison with expected values (Fig. 2a). Early-stage precipitation during hydration/hydroxylation of CO_2 has previously been proposed as a primary driver of disequilibrium in the dual clumped isotope composition of coral and brachiopod carbonate[60,66]. However, disequilibrium offsets in Δ_{47}–Δ_{48} values of LBF calcite are substantially smaller than those observed in corals and brachiopods. Combined with uncertainties in growth temperatures, this limits our ability to identify correlated Δ_{47} and Δ_{48} disequilibrium trajectories.

Experimental work on the LBF *A. lobifera* demonstrates that ion supply to the calcifying surface is driven by seawater endocytosis and transport in vacuoles[67,68]. In the enclosed microenvironment of the seawater vacuole, pH is up-regulated through proton export, increasing DIC concentration and Ω[68–70]. CO_2, likely concentrated and supplied by small acidic vesicles[68], is then drawn into the vacuole, along a pCO_2 gradient, where it is converted to HCO_3^-. Isotopic equilibration between dissolved CO_2 and HCO_3^- through (de)hydration/(de)hydroxylation reactions occurs relatively slowly compared with other reactions in the DIC-H_2O-CO_2 system[71]. In high-Mg calcite biomineralizing foraminifera, including *A. lobifera* and *O.*

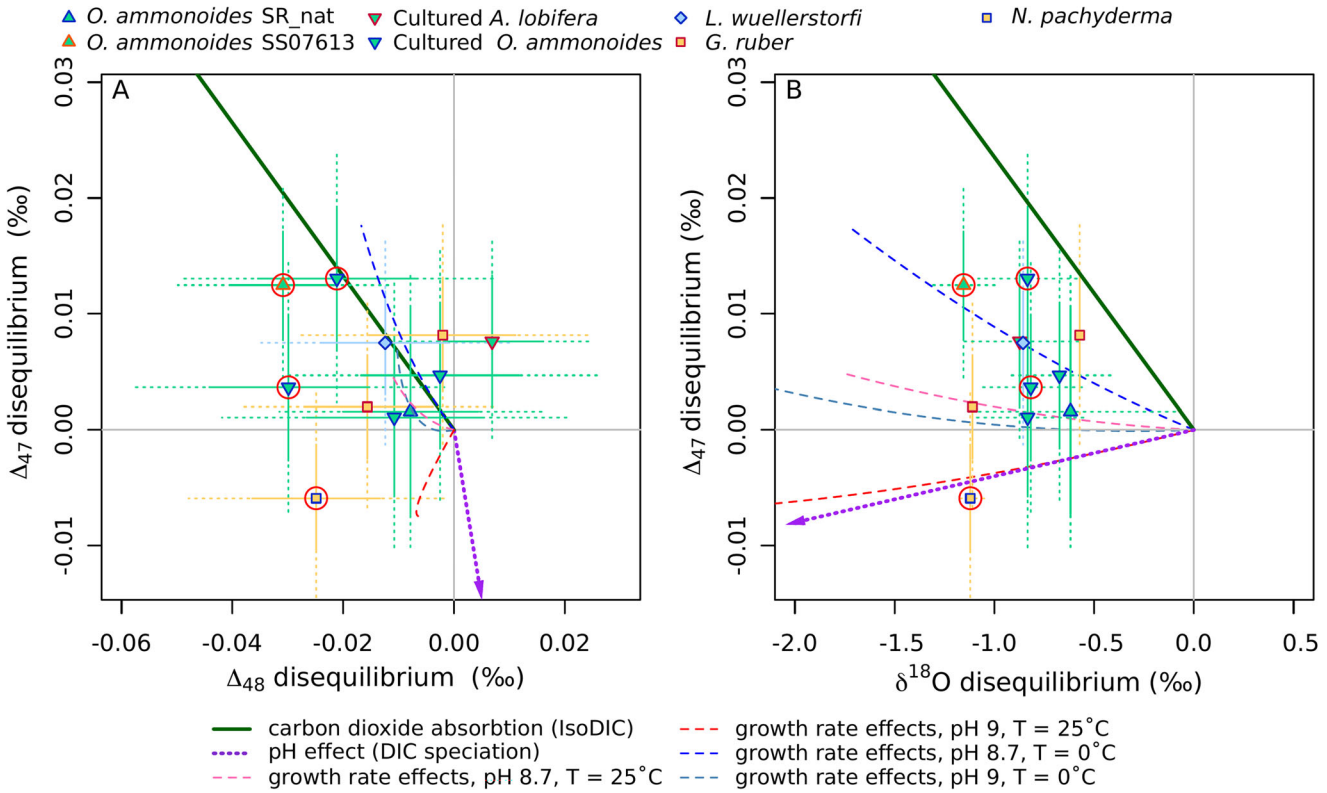

Fig. 2 | Disequilibrium isotope offsets in Δ_{47}, Δ_{48} and $\delta^{18}O$ of foraminifera. a The dual clumped isotope composition of foraminifera, where disequilibrium offset is calculated based on measured Δ_x–expected Δ_x (calculated based on known or WOA based growth temperatures using calibration of Fiebig et al.,[55] where x is mass 48 or 47). The expected Δ_x for mixed cultured *O. ammonoides* reflects growth weighted natural growth and culture temperatures (Eq. 1, Supplementary Table 3). **b** plot of disequilibrium $\delta^{18}O$ vs. disequilibrium Δ_{47} (relative to Coplen[62] and Fiebig et al.[55], respectively). In Figures (**a**) and (**b**) IsoDIC predicted disequilibrium Δ_{47}/Δ_{48} and $\Delta_{47}/\delta^{18}O$ trajectories during early-stage CO_2 absorption in foraminifera are plotted as green lines. Also shown are disequilibrium trajectories induced by attachment/detachment kinetics[90,9190,91], modelled as a function of growth rate (0 and 10^{-4} mol m^{-2} s^{-1}), pH and temperature (see legend for details). The predicted linear trajectories of disequilibrium isotope evolution associated with DIC speciation[87] on pH up-regulation are shown as purple dashed lines. Errors are presented at the 68% (solid error bars) and 95% (dashed error bars) confidence levels and include full propagation including calibration and growth temperature uncertainties. Samples circled in red plot distinguishable from Δ_{47}-Δ_{48} equilibrium at the 95% Cl. See Supplementary Fig. 3 for disequilibrium offsets in core-top samples plotted in comparison with species-specific T_{18} growth temperature estimates.

ammonoides[72,73], $CaCO_3$ may be precipitated in vacuoles as an intermediate amorphous phase (ACC) or vaterite[74,75] before its final transformation to calcite.

We studied the extent of Δ_{47}- and Δ_{48}-disequilibrium that can be introduced by the rate-limiting nature of the slow (de)hydration/(de)hydroxylation reactions using the IsoDIC model[76] (Fig. 2a). This model simulates temporary evolution of isotopic disequilibrium bias in dissolved bicarbonate during exposure of an equilibrated DIC solution to a CO_2-containing atmosphere, prior to the onset of carbonate precipitation. Disequilibrium bias originates from incomplete (de)hydration/(de)hydroxylation reactions and can be expected to be transferred 1:1 into the precipitated carbonate provided precipitation itself proceeds without any superposed kinetic isotope effect. We ran the IsoDIC model for the boundary conditions characteristic of the growth of photosymbiotic LBF; [DIC] = 2 mM; temperature of 24 °C, pH of 8.7 and $\delta^{13}C$ of −8 ‰[69,77] (further details in Supplementary Methods 1). Model outputs indicate a Δ_{47}/Δ_{48} disequilibrium offset slope for early-stage CO_2 absorption of approximately −0.7, characteristic of mixing of HCO_3^- kinetic endmember produced by the early-stage hydration/hydroxylation of CO_2 with an equilibrium HCO_3^- endmember derived from seawater. All LBF plot within error of IsoDIC model predicted Δ_{47}/Δ_{48} co-evolution at 95% Cl. The observed agreement between model-predicted and measured extents of disequilibrium may therefore indicate that LBF inherit their Δ_{47}–Δ_{48} disequilibrium signatures directly from the dissolved bicarbonate. The IsoDIC predicted $\delta^{18}O/\Delta_{47}$ disequilibrium offset slope for early-stage CO_2 absorption, however, does not align with observed $\delta^{18}O/\Delta_{47}$ offsets in foraminifera (Fig. 2b), indicating that another process may contribute to disequilibrium offsets in the isotope composition of LBF calcite, particularly for $\delta^{18}O$.

Early studies on the stable isotope composition of foraminifera highlighted an alternative explanation for the generation of isotopic disequilibrium bias in foraminiferal calcite. In these studies, a link between $\delta^{18}O$ values of planktic foraminifera, carbonate ion concentration [CO_3^{2-}] and pH local to the foraminiferal test[11,15,16,78] was observed. More recent research suggests a similar relationship between the $\delta^{18}O$ composition of benthic foraminiferal carbonate and local [CO_3^{2-}][13,79,80]. This would have implications for paleo-applications as it suggests that local seawater pH can impact foraminiferal oxygen isotope temperature reconstruction, and should also be estimated, especially where large variations in pH might be expected[81–84]. The observed relationship between $\delta^{18}O$ values of foraminiferal carbonate and pH may be explained if isotopically equilibrated chemical species HCO_3^- and CO_3^{2-} are precipitated from the calcifying solution in variable proportions, without any superposed kinetic isotope effect. Each species has a unique equilibrium oxygen isotope fractionation factor with respect to water at a given temperature. Thus, changes in the relative proportions of HCO_3^- and CO_3^{2-}, driven by pH change, lead to changes in the oxygen isotope composition of forming carbonate[85–87]. Experimental studies suggest a ~ 7 ‰ difference in oxygen isotope fractionation factors between HCO_3^- and water, and CO_3^{2-} and water, respectively, at environmental temperatures[85]. The Δ_{64} of CO_3^- is predicted to be 0.012 ‰ higher than that

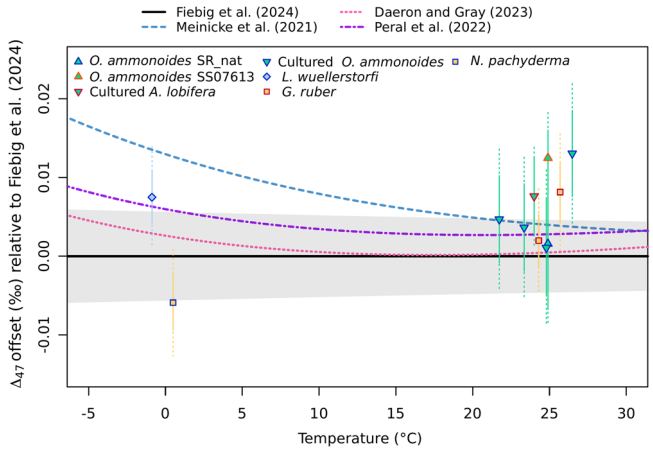

Fig. 3 | Δ_{47} offsets of samples measured in this study and foraminiferal calibrations relative to assumed empirical equilibrium. Offset in Δ_{47} for recent foraminiferal Δ_{47}-temperature calibrations and foraminifera measured in this study relative to empirical equilibrium[55]. Δ_{47} offsets are calculated based on measured Δ_{47} – expected Δ_{47} (calculated based on known or WOA based growth temperatures using calibration of Fiebig et al.[55]). The expected Δ_{47} for mixed cultured *O. ammonoides* reflects growth weighted natural growth and culture temperatures (Eq. 1, Supplementary Table 3). Sample errors are presented at the 68% (solid error bars) and 95% (dashed error bars) confidence levels, including propagated error on Δ_{47}. The shaded area represents 95% confidence interval on the equilibrium calibration[55] calibration error is thus not propagated onto sample errors.

of HCO_3^- at 25 °C, while the Δ_{63} CO_3^{2-} is predicted to be 0.033 ‰ lower[56]. Changes in DIC speciation are therefore associated with a theoretically predicted Δ_{47}/Δ_{48} disequilibrium correlation slope of approximately -2.79[56,76], assuming the isotopic composition of DIC (i.e., CO_3^{2-} and HCO_3^-) is quenched during $CaCO_3$ formation. Increases in pH at the site of calcification in foraminifera has been demonstrated for several foraminiferal species[68,69,77]. Rising pH increases the ratio of CO_3^{2-} to HCO_3^- in solution. Therefore, pH up-regulation is predicted to correspond to enrichments in Δ_{48} and depletions in $\delta^{18}O$ and Δ_{47} relative to empirical equilibrium[55]. While $\delta^{18}O$ is depleted in comparison with empirical equilibrium of[57,62] foraminifera exhibit depletions in Δ_{48} and enrichments in Δ_{47} relative to empirical equilibrium[55] (Fig. 2a). Consequently, the speciation effect is unlikely to be the only driver of isotopic disequilibrium in foraminiferal carbonate, and there is no evidence to support a pH correction on foraminiferal Δ_{47}. It is not possible, based on measured data, to resolve the effect of pH on foraminiferal $\delta^{18}O$ values.

Watkins and Hunt[88] proposed that both kinetic isotope effects occurring at the solution-crystal interface and the DIC speciation effect should be considered to account for the oxygen isotope disequilibrium patterns observed in foraminifera. In their ion-by-ion growth model, equilibrated DIC-species HCO_3^- and CO_3^{2-} are attached and detached to the carbonate surface during crystal growth. At the kinetic limit of high growth rates, attachment occurs much faster than detachment such that the corresponding kinetic oxygen isotope fractionations associated with the attachment reactions of HCO_3^- and CO_3^{2-} are fully expressed in the precipitated carbonate. At slow growth rates, the detachment rate approaches the attachment rate such that equilibrium fractionations are expressed. This model was more recently updated to describe expected Δ_{47}-Δ_{48} disequilibrium patterns at the kinetic limit[89]. The pH, temperature and growth rate dependent disequilibrium Δ_{47}-Δ_{48} vectors characteristic of attachment/detachment kinetics for growth rates between 0 and 10^{-4} mol m^{-2} s^{-1} (approaching the kinetic limit) are also shown in Fig. 2a. Modelled disequilibrium offsets are relatively small in magnitude in comparison with the Δ_{47} offsets in *O. ammonoides* from the great barrier reef and cultured sample SR50_4LBF but agree, within error with offsets in foraminiferal Δ_{47}, Δ_{48} and $\delta^{18}O$ values (Fig. 2). The magnitude of Δ_{47}-Δ_{48} disequilibrium trajectories in the model of Watkins and Devriendt[89] depends on the constraint on the isotopologue specific kinetic fractionation factors included in the model, and true offsets could be larger. We therefore conclude that while kinetic fractionation during CO_2 absorption is likely the primary driver of dual clumped isotope disequilibrium in LBF, a contribution from kinetically controlled precipitation cannot be excluded.

Eocene temperatures in the Hampshire and Paris Basins and outlook for paleoclimate reconstruction using Large Benthic Foraminiferal Δ_{47}

All fossil *Nummulites* samples are characterised by Δ_{47}-Δ_{48} values that are within 95% Cl of dual clumped isotope equilibrium (Fig. 1). Direct projection of Δ_{47} to the empirical equilibrium Δ_{47}-T relationship[55] yields a seawater temperature range of 25.2 ± 3.0 °C to 29.1 ± 3.1 °C, reflecting Eocene warmth at the paleolatitude of measured samples (~45°N). Modern LBF do not show well correlated patterns of disequilibrium in Δ_{47} and Δ_{48}. That is, they do not align well along a single disequilibrium trajectory (Fig. 2a). Dual clumped isotope correction along the IsoDIC predicted slope of -0.7 therefore results in poor estimates of corrected growth temperatures, particularly for samples plotting indistinguishable from Δ_{47}-Δ_{48} equilibrium (Supplementary Fig. 2). As a result, we do not correct the dual clumped isotope composition of Eocene LBF for kinetic bias. Because modern LBF that fall within Δ_{47}–Δ_{48} equilibrium (95% CI) may exhibit a slight positive Δ47 bias (Fig. 2a), Δ_{47}-derived temperatures should be regarded as minimum estimates. Clumped isotope (Δ_{47}) derived temperatures for Ypresian LBF from the Paris basin, measured in this study, are 27.5 ± 3.1 °C and 25.2 ± 3.0 °C for samples of ages 50.6-51.2 Ma and 51–52 Ma, respectively. These temperatures concur with oxygen isotope paleotemperatures of 25 °C to 32 °C (with average of 27 °C) for Ypresian oysters and volutids of the Paris basin[90]. Temperatures reconstructed from Lutetian LBF collected from the Hampshire basin are 27.9 °C ± 3.1 °C and 29.1 °C ± 3.1 °C for 46-47 Ma and 42.5-45 Ma, respectively. Temperatures reported here are also consistent with previously published clumped isotope temperatures of 28.5–31.1 °C from measurements of Eocene LBF[28] of the Hampshire and Belgium basins and 33 °C ± 4.4 °C from dual clumped isotope measurement of the bivalve *Venericor planicosta*[91] from the Paris Basin, thought to have grown during the Mid-Eocene Climate Optimum[92].

The congruence between reconstructed Eocene temperatures from fossil LBF and previous paleotemperature reconstructions[28,90,91] may indicate that fossil LBF with Δ_{47}-Δ_{48} values within error (2 SE) of empirical equilibrium are promising Δ_{47} archive. However, some modern LBF plot distinguishable from Δ_{47}-Δ_{48} equilibrium[55] (at 95% Cl) (Fig. 1) and exhibit temperature offsets to cooler temperatures than measured growth temperatures (Fig. 3). Therefore, caution is warranted when applying the clumped isotope thermometer to LBF. Dual clumped isotope analysis provides a useful method to screen for large kinetic departures from dual clumped isotope equilibrium in fossil LBF. Samples plotting distinguishable from equilibrium at 95% Cl should be discounted from temperature reconstructions or interpreted only within the framework of group or species-specific empirical calibrations. Whenever possible, temperatures reconstructed by LBF-Δ_{47} may be checked independently by measurement of co-eval specimens from other groups with equilibrium Δ_{47}-temperature relationships, such as bivalves[93]. Further measurement of modern LBF across a broader range of growth temperatures could help clarify Δ_{47}-Δ_{48} patterns, enhance our understanding of kinetic controls on biomineralization and enable robust dual clumped isotope temperature reconstructions from fossil samples, without the need for group-specific calibrations[13].

Comparison with previous studies and perspective for the use of core-top foraminiferal Δ_{47}

Observed disequilibrium in some LBF contrasts with previously reported Δ_{47}-temperature relationships consistent with equilibrium in core top planktic and benthic foraminifera[35,39,45]. Our dual clumped isotope measurements of core-top foraminifera plot within error of empirical Δ_{47}-Δ_{48}[55] equilibrium at the 95% Cl (Fig. 1). Furthermore, Δ_{47} values of all core-top

foraminifera agree with accepted WOA18 + FAME calcification temperatures if uncertainties associated with assumed calcification temperatures and on the Δ_{47}-temperature calibration are considered (Fig. 2). Application of the empirical calibration[55] to our dataset yields Δ_{47} temperatures within 2.9 °C of WOA18 + FAME temperatures. Although a slight Δ_{48} disequilibrium bias seems to be indicated for *N. pachyderma* (Fig. 2a), such negative bias is not statistically significant across the small population ($n = 3$) of all planktic foraminifera. Apparent absence of significant Δ_{47} offsets and temperature offsets from WOA18 derived growth temperatures (Fig. 3) reflects the reasonable agreement shown in previous studies between salinity and pH corrected Mg/Ca temperatures and Δ_{47} based temperatures[40,44] as well as between Δ_{47} and species-specific $\delta^{18}O$-based temperature estimates[45].

Previous studies adopted $\delta^{18}O$ derived growth temperatures (T_{18}), applying empirical calibration equations[64,65] or species-specific fractionation relationships[20–22]. Species specific $\delta^{18}O$-derived growth temperature estimates (T_{18}) for planktic foraminifera[21,45] yield statistically significant disequilibrium Δ_{47} offsets in *G. ruber* and *N. pachyderma* (Supplementary Fig. 3). The definition of $\delta^{18}O$ derived growth temperatures (T_{18}) based on empirical calibration equations[64,65] or species-specific fractionation relationships[20–22] relies on the assumption of empirical $\delta^{18}O$-temperature relationships that accurately account for observed disequilibrium in foraminiferal $\delta^{18}O$ (Fig. 2b). This approach may therefore introduce error into Δ_{47}-temperature calibrations. For example, the $\delta^{18}O$ derived growth temperature estimates calculated using the species-specific calibration of Mulitza et al.[21], reprocessed after Däeron and Gray[45] for *G.ruber* measured in this study are ~4 °C colder than Δ_{47} derived temperatures based on the equilibrium calibration[55] despite these samples plotting within 95% CI of dual clumped isotope equilibrium. The species-specific T_{18} estimates are also 4.5 ± 0.1 °C for sample MD96-2048_3 and 7.1 ± 0.1 °C for sample M1125-72-2 colder than FAME-WOA18 derived temperatures. Integrating these species specific $\delta^{18}O$ derived temperatures into the FAME model yields unrealistically deep calcification depths for *G. ruber*, a photosymbiotic species. The diagenetic overprinting of secondary carbonate in deeper waters may be used to explain T_{18} and Δ_{47} values that co-vary to lower temperature but does not explain the significant difference between Δ_{47} derived temperatures and T_{18} in *G. ruber*.

Based on the analysis of three planktic and a single small benthic foraminifera sample(s) we do not have indication that the clumped isotopic composition of these archives is susceptible to significant disequilibrium bias. However, larger populations of these groups need to be analysed to confirm these very preliminary results. It remains unclear whether a single biomineralization model applies to planktic foraminifera, deep-sea benthic foraminifera and LBF, such that biogenically driven non-equilibrium effects would be similarly expressed across them. Three of four measured core-top samples, planktic foraminifera *G. ruber* and *N. pachyderma* and benthic *L. wuellerstorfi*, exhibit offsets in Δ_{47}-Δ_{48} at the 68% CI in comparison with the equilibrium calibration[55], in the same direction as offsets observed in LBF (Fig. 1). The overall pattern of depletion in Δ_{48} observed in all measured foraminifera, except for *A. lobifera*, contrasts with observed Δ_{47}-Δ_{48} relationships in biomineralizing organisms such as of modern molluscs, assumed to precipitate in clumped isotope equilibrium[93] which show both enrichment and depletion in Δ_{48} in comparison with equilibrium[55]. When scaling the inorganic dual clumped isotope calibration of Swart et al.[94], consisting of seven carbonate samples with growth temperatures between 5 and 65 °C, to the fourth-order theoretical Δ_{47}-temperature relationship[56], the Fiebig et al.[55] and Swart et al.[94] calibrations plot within 5 ppm of each other in Δ_{48} within the temperature range of foraminifera measured in this study. Thus at present, we have no reason to believe that inaccuracies in the equilibrium Δ_{48}-temperature relationship[55] drive the pattern of minor offsets in foraminiferal Δ_{47}-Δ_{48} relationships in comparison with the empirical equilibrium of Fiebig et al.[55]. If minor offsets in Δ_{47}-Δ_{48} in foraminiferal calcite reflect kinetic effects driving Δ_{47} to lower temperatures, these offsets may effectively be accounted for by applying group-specific empirical calibrations. The calibration of Peral et al[44]. plots within error and with a similar temperature dependence to the calibration of Fiebig et al[55]. although it yields Δ_{47} derived temperatures that are on average 1 °C warmer (Fig. 3). In contrast, the calibration of Meinicke et al[26]. deviates from the calibration of Fiebig et al[55]. at low temperatures, yielding clumped isotope derived temperatures ~3.9 °C warmer at 0 °C and ~1.4 °C warmer at 25 °C (Fig. 3).

The deep-sea benthic *L. wuellerstorfi* (Figs. 1, 2a) is characterised by the same average offset from dual clumped isotope equilibrium as planktic foraminifera *G. ruber* and *N. pachyderma*. This observation does not reflect the suggested offset in the Δ_{47}-temperature relationships of benthic foraminifera[35,46] and planktic foraminifera[35,39] most recently discussed in Däeron and Gray[45]. The Δ_{47} value of *L. wuellerstorfi* presented in this study agrees within 4ppm with the Δ_{47} value for the same sample, presented in Peral et al.[35]. This corresponds to a reconstructed temperature of −3.2 ± 2.6 °C (2 SE), which agrees within error with a bottom water temperature of −0.9 ± 0.1 °C. Apparent attainment of equilibrium contrasts with apparent offsets in the benthic dataset of Piasecki et al.[46] which, reprocessed to the ICDES[45], shows enrichment in Δ_{47} in comparison with empirical equilibrium[45,55].

Conclusion

We report disequilibrium in the dual (Δ_{47}-Δ_{48}) clumped isotope compositions of some LBF of species *Operculina ammonoides*. The observed isotopic disequilibrium likely relates to carbonate precipitation from a slightly disequilibrated DIC pool during early-stage hydration/hydroxylation of CO_2. LBF *O. ammonoides* that plot with distinguishable offsets from dual clumped isotope equilibrium yield Δ_{47} based reconstructed growth temperatures that are colder than measured growth temperatures when equilibrium Δ_{47}-temperature calibrations[55] are applied. However, some LBF plot consistent with Δ_{47}-Δ_{48} equilibrium, yielding Δ_{47}-temperatures within error of measured growth temperature. Thus, when sample size permits dual clumped isotope measurement is a valuable tool for identifying disequilibrium precipitation in LBF. Application of the dual clumped isotope thermometer to Eocene *Nummulites* from the Paris and Hampshire basins yielded Δ_{47}-Δ_{48} values consistent with equilibrium[55] at 95% CI, enabling the reconstruction of Δ_{47}- temperatures that reflect previously reported Eocene warmth (~25–29 °C) in the region[28,90,91]. Equilibrium Δ_{47}-temperature relationships cannot be reliably applied to LBF that are offset from empirical dual clumped isotope equilibrium (95% CI), therefore, these samples require empirical calibration. Further measurements of Δ_{47}-Δ_{48} offsets in LBF may help to identify patterns in dual clumped isotope disequilibrium which could be used to correct for kinetic effects in Δ_{47}.

Dual clumped isotope values of core-top low-Mg foraminifera plot within error of empirical Δ_{47}-Δ_{48} equilibrium[55] at the 95% CI. At this point, we find no indication of significant kinetic bias in their clumped isotopic compositions. However, three of four core-top samples (the planktic foraminifera *G. ruber* and *N. pachyderma* and the benthic *L. wuellerstorfi*) plot distinguishably from dual clumped isotope equilibrium at 68% CI, reflecting the pattern of Δ_{47}-Δ_{48} offsets observed in LBF (Fig. 1), although we note the small number of dual clumped isotope measurements of core-top foraminifera presented in this study ($n = 4$). Further measurements of Δ_{47}-Δ_{48} in core-top foraminifera, encompassing both planktic and benthic taxa, are required to assess whether systematic differences exist between the dual clumped isotope signatures of planktic foraminifera, benthic foraminifera, and empirical equilibrium, and to evaluate whether such differences introduce bias into Δ_{47}-based reconstructions of foraminiferal calcification temperatures.

Methods

Sample details and preparation

Planktic foraminifera originate from three core-tops with varying latitudes and growth temperatures. Sampling location details, species and approximate core top ages are shown in Supplementary Table 5. The deep-sea benthic sample MOCOSED_2014_1 of species *Lobatula wuellerstorfi* and planktic samples of *Neogloboquadrina pachyderma s.*, (MOCOSED_2014_2) are originally described in Peral et al.[35] and

Globigerinoides ruber s.s. (MD96-2048) described in Caley et al.[95] and originally measured in Peral et al.[96]. Details of core-top age determination for sample MD96-2048 are given in Supplementary Methods 2. In some publications, including Peral et al.[35], *Lobatula wuellerstorfi* is reported as *Cibicidoides wuellerstorfi*. According to the WoRMS database (https://www.marinespecies.org/index.php), this species is currently classified as *L. wuellerstorfi*. Benthic foraminifera *L. wuellerstorfi* (MOCOSED_2014_1) were sampled from the same core as planktic foraminifera *N. pachyderma s.* (MOCOSED_2014_2). *Globigerinoides ruber* (white and pink (w + p)) sample M125_72_2 originates from a core-catcher sample retrieved during RV Meteor expedition M125 in 2016 offshore Brazil[97].

LBF were both field collected (sample SS07G13 and SR_nat) and cultured at the Hebrew University of Jerusalem (samples SR50_1LBF, SR50_2LBF, SR50_3LBF, SR50_4LBF and MS1FO). *Operculina ammonoides* sample SS07G13 was collected on the Great Barrier Reef[98]. The clumped isotope composition (Δ_{47}) of this sample was previously measured by Evans et al[28]. and assigned calcification temperature of 24.7 ± 0.8 °C based on World Ocean Atlas (WOA) temperatures[99]. *Amphistegina lobifera* sample MS1FO was maintained at the same temperature (24.0 ± 1.5 °C) throughout the whole LBF growth period, at the Hebrew University of Jerusalem. Samples were crushed using a mortar and pestle and sample powder was stored in a desiccator prior to analysis, samples consisted of several homogenised individual specimens.

Culture experiments utilized LBF (*Operculina ammonoides*) collected from the Gulf of Eilat (GOE) north shore (29.5363 °N, 34.9668 ° E) from a depth of 20-30 meters on the 12.8.2021 (sample SR_nat, growth temperature 24.7 ± 2.7 °C based on long-term measured seawater temperature data for the Northern Gulf of Eilat). SR_nat formed the starting material and control for the culture, its isotopic composition was independently measured. Culture experiments were carried out at the Hebrew University of Jerusalem. The sediment was sieved between 200 µm to 1000 µm and live foraminifera were identified as those that climbed glass slides. Foraminifera (size 345 µm to 691 µm) were counted, totaling 100 individuals per experiment, placed into 130 ml sealed glass jars with filtered seawater (average $\delta^{18}O$ of 2.01 ‰) and incubated in temperature-controlled water baths at 19.3, 22.1, 24.9, and 28.0 °C with a temperature tolerance of ± 0.2 °C. Two cultures were made for each temperature. Water was replaced once a week and sampled for oxygen isotopes, pH and alkalinity. Two methods were used to calculate percentage of new growth (f) under culture conditions: (1) calculation of new growth fraction by alkalinity change over the culture period and (2) calculation of new growth fraction by mass increase[100]. Initial mass was determined by drying and weighing a control group of specimens (size 345–691 µm). At the end of the experiment the foraminiferal aliquots were washed 5 times with distilled deionized water (DDW), oven dried at 50 °C, pre-treated with 10% NaOCl for 12 hours, washed five times with DDW and dried at 50 °C for 3 days, weighed and counted[101]. Following the discussion of Hauzer et al.[72], in this study we apply values calculated by alkalinity change. On average, samples exhibited 75–102% new growth over the culture period corresponding to 42–51 % new calcite grown at culture temperature. A summary of growth data for cultured foraminifera is given in Supplementary Table 3. All samples, consisting of several individual specimens to make up >50 mg of carbonate, were powdered using a mortar and pestle prior to clumped isotope analysis.

Nitrate contamination in biogenic carbonates has been inferred to impact Δ_{47} and Δ_{48} values through the production of NO_2 gas during acid digestion, which acts as an isobaric contaminant on m/z 47 and 48[55]. Isobaric interference associated with $NO2^+$ in the ion source causes enrichment in Δ_{48} and Δ_{47} depletion relative to equilibrium. We therefore bleached an aliquot of sample MF1SO (which has the most positive Δ_{48} in comparison with Δ_{47}-Δ_{48} equilibrium) with 3 % NaOCl as described in Fiebig et al.[55] to assess the potential for nitrate contamination. The measured difference between bleached (19MS1FO_a, $n = 13$) and unbleached (19MS1FO_b, $n = 5$) aliquots was only 0.002 ‰ for Δ_{47} and 0.005 ‰ for Δ_{48}, within analytical error, indicating that nitrate contamination does not bias the dual clumped isotope composition of foraminiferal calcite. These findings are consistent with earlier measurements[28], which showed no significant difference in Δ_{47} between pre-treated and untreated fossil and modern LBF. Thus, aliquots 19MS1FO_and 19MS1FO_b were pooled, treated as one sample (MS1FO), and all other foraminiferal samples were not oxidatively cleaned (apart from SS07G13, see Evans et al.). Samples MOCOSED_2014_1, MOCOSED_2014_2, and MD96-2048 were prepared by rinsing at least twice in ultrapure water in an ultrasonic bath for 1 min, then rinsed twice with reagent-grade methanol in an ultrasonic bath for 30 seconds[35].

Eocene LBF (*Nummulites* sp.), with ages between 46 and 52 Ma were collected from the Paris and Hampshire basins[92,102–104]. Sampling locations, species and approximate age are shown in Supplementary Table 2. Samples from the Earnley Sand Formation at Whitecliff Bay (Isle of Wight, UK) were collected during low tide, when the formation is exposed along the beach. The preservation of the fossil samples was verified by SEM imaging and trace element analysis using LA-ICPMS. Samples showing high Al/Ca values (>0.5 mmol/mol) or evidence of recrystallization with statistically significantly lower Mg/Ca and Sr/Ca values were excluded to minimize the effects of diagenetic alteration[105]. Samples were sonicated in deionised water to remove any coating sediment, dried in a vacuum at room temperature and crushed using a mortar and pestle. Each sample consists of a single specimen (>100 mg carbonate).

Estimation of calcification temperatures

Though the dual clumped isotope approach does not require a priori knowledge of growth temperature to identify kinetic departures from equilibrium, we estimate calcification temperatures to assess patterns in disequilibrium Δ_{47} and Δ_{48} values and to evaluate the degree to which Δ_{47}-derived temperatures for foraminifera measured in this study reflect calcification temperatures.

WOA-based and directly measured temperatures

Estimated calcification temperatures are based on the 2018 World Ocean Atlas temperatures (1/4° grid) (WOA 18; Locarini et al.[59]). In the case of planktic foraminifera, the Foraminifera as Modelled Entities (FAME)[101] module, with hydrographic temperature fields derived from WOA18 (at 1/4° resolution), is used to calculate calcification temperatures. FAME is a foraminiferal growth module, developed in Python. The module forecasts the presence or absence of commonly used planktic foraminifera and their expected calcification temperatures. It uses a very limited number of parameters, almost all derived from culture experiments[106].

We use the FAME module to predict the calcification temperatures of foraminifera, accounting for seasonal and depth variations in specific foraminiferal habitats as described in Roche et al.[101]. FAME predicts mean calcification temperature of a foraminiferal sample, composed of multiple individuals, by weighting oceanic conditions according to individual growth rates across space (depth in the water column) and time (months) (Supplementary Fig. 4). In the case of benthic species *L. wuellerstorfi*, we use the mean WOA18 annual bottom water temperature at the site of collection. FAME predicted global calcification temperature maps for *G. ruber* and *N. pachyderma* and seasonal temperature-depth profiles reconstructed from WOA18 data for core-top sites are shown in Supplementary Figs. 5–7. The growth temperature for large benthic foraminifera sample MFS1O, grown in a stock aquarium, is based on direct measurements of aquarium temperature.

$\delta^{18}O$-derived calcification temperatures (T_{18})

In line with studies that conclude that $\delta^{18}O$-derived temperatures may be better at estimating calcification temperature of foraminifera owing to uncertainties associated with imperfect knowledge of foraminifera ecology[35,39,45], we also calculate and present $\delta^{18}O$-derived calcification temperatures (T_{18}) based on measured $\delta^{18}O_{carbonate}$ and annual resolution[107]. We calculate $\delta^{18}O$-derived calcification temperatures based on Kim and O'Neil[64] adjusted to an acid fractionation factor of 1.010254[108] and species

specific foraminiferal $\delta^{18}O$-carbonate calibrations for *G. ruber*, *L. wuellerstorfi*, and *N. pachyderma*[45]. $\delta^{18}O$-derived estimates of calcification temperature are presented in Supplementary Table 4.

Culture experiments

Assessing the growth temperature of cultured foraminifera is complicated as these samples consist of a mixture of material precipitated both prior to collection and in the laboratory. Expected Δ_{47} was estimated based on mixing of two endmember calcites: the starting composition of the control group (SR_nat), which we independently measured, and newly grown calcite under temperature-controlled culture. We first explored the effects of non-linear mixing in Δ_{47}/Δ_{48} space using mixing calculations which follow equations 19, 20, 21 and 27 in Guo (2020). Expected Δ_{47} and $\delta^{18}O$ of end member calcites were calculated based on assumed growth temperature and measured $\delta^{18}O_{water}$, while the $\delta^{13}C$ of the cultured endmember was based on the endmember composition of the control sample (SR_nat) and the $\delta^{13}C$ of mixed cultured-natural powdered samples. Over the maximum difference between endmembers (1.3 ‰ in $\delta^{18}O$ and 4.6 ‰ in $\delta^{13}C$) mixing effects correspond to maximum enrichments of 0.002 ‰ in Δ_{47} and 0.001 ‰ in Δ_{48} and thus can be ignored.

The assumed growth temperature of mixed samples can also be calculated based on fractional percentage of new growth at culture temperature (Eq. 1).

$$T_{mix} = (1-f) \times T_{original} + f \times T_{culture} \quad (1)$$

Error on assumed growth temperature T_{mix} includes analytically propagated error on fraction of new growth at culture temperature (f), error on $T_{original}$ and error on $T_{culture}$ as shown in Supplemenatry Table 5.

IRMS measurement and data processing

Isotopic analyses were carried out at the Stable Isotope Laboratory at Goethe-University Frankfurt following the analytical setup and methodology described in detail in Fiebig et al.[52] and Bernecker et al.[54]. Dual clumped isotope (Δ_{47} and Δ_{48}), $\delta^{18}O$ and $\delta^{13}C$ values are measured simultaneously on the same analyte CO_2, using a Thermo Scientific 253 Plus mass spectrometer coupled to the custom front-end peripheral HAL for acid digestion of 10.0 ± 0.2 mg carbonate samples using 108 wt% H_3PO_4 at 90 °C[52]. Measurements of analyte CO_2 were made at 16,000 ± 100 mV on m/z 44, in 13 acquisitions, each comprising 10 cycles with an integration time of 20 s, totalling an integration time of 2600 s per replicate.

CO_2 standards equilibrated to 25 °C and 1000 °C with three distinct bulk isotope compositions were measured alongside samples[54] facilitating translation to the Carbon Dioxide Equilibration Scale (CDES)[109] and correction for mass spectrometric non-linearity through the iterative derivation of scaling factors[54]. Optimal scaling factors were calculated based on measured m/z 47.5 intensities such that δ_{47} vs Δ_{47} and δ_{48} vs Δ_{48} of gasses equilibrated to 25 °C and 1000 °C have slopes indistinguishable from 0. Background-corrected raw data are standardised with D47crunch[58] using equilibrated gas standards as anchors and a pooled session approach applying drift correction and variance minimization over unknowns and anchors, assigning Δ_{47} values of 0.9196 ‰ and 0.0266 ‰ and Δ_{48} values of 0.345‰ and 0 ‰ for CO_2 equilibrated at 25° and 1000 °C, respectively[52,110]. Background correction and standardization was achieved using D4Xgui[111]. Final Δ_{47} and Δ_{48} values are reported on the CDES90. Replicate sample measurements were temporally spread within sessions. ETH-1, ETH-2 and ETH-3 were also analysed, but not used as anchors for clumped isotope correction, with one standard measured every two to three samples. The long-term value of ETH1 is 0.2071 ‰ ($n = 584$) and ETH2 is 0.2094 ‰ ($n = 575$) and the long-term standard deviation on these two measurements is 0.0090 ‰ and 0.0085 ‰, respectively. $\delta^{18}O$ and $\delta^{13}C$ were also standardised in D47crunch[58] using samples ETH-1 and ETH-2 as anchors. Fiebig et al.[55] recently determined that ETH-3 Δ_{47} and Δ_{48} data made at Goethe-University Frankfurt before January 2024 was compromised by the presence of ppb concentration traces of NO_2 in the analyte CO_2. Since ETH-3 constitutes a significant fraction (8 %) of all data and variance minimization of compromised ETH-3 samples may affect determination of correction parameters a, b and c (see equation 18 in ref. 58), we excluded ETH-3 from the variance minimization algorithm of Δ_{47} by providing individual identifiers to each ETH-3 replicate[55].

To determine statistical differences between the empirical equilibrium Δ_{47}-Δ_{48} relationship[55] and Δ_{47}-Δ_{48} of foraminiferal carbonate we applied Welch's T-test to two groups. Groups consisted of disequilibrium offsets calculated as Δ_{48} offset from the equilibrium relationship[55] at Δ_{47}-derived temperatures of (1) inorganic carbonates used for empirical calibration and of (2) foraminiferal group of interest. The use of Welch's T allows for unequal variance between groups. Tests are reported in APA style[112].

Reporting summary

Further information on research design is available in the Nature Portfolio Reporting Summary linked to this article.

Data availability

Data, extended methods and Supplementary Figs. belonging to this study are available in the open-access database Zenodo, https://doi.org/10.5281/zenodo.20594013[113]. This online database contains the following supplementary data files:

Received: 8 October 2025; Accepted: 14 June 2026;
Published online: 08 July 2026

References

1. Urey, H. C. Oxygen isotopes in nature and in the laboratory. *Science* **108**, 489–496 (1948).
2. Zachos, J., Pagani, M., Sloan, L., Thomas, E. & Billups, K. Trends, rhythms, and aberrations in global climate 65. *Ma Present. Sci.* **292**, 686–693 (2001).
3. Veizer, J. & Prokoph, A. Temperatures and oxygen isotopic composition of Phanerozoic oceans. *Earth. Sci. Rev.* **146**, 92–104 (2015).
4. Gaskell, D. E. et al. The latitudinal temperature gradient and its climate dependence as inferred from foraminiferal δ 18 O over the past 95 million years. **119**, (2022).
5. Lisiecki, L. E. & Raymo, M. E. A Pliocene-Pleistocene stack of 57 globally distributed benthic δ18O records. *Paleoceanography* **20**, 1–17 (2005).
6. Waelbroeck, C. et al. Sea-level and deep water temperature changes derived from benthic foraminifera isotopic records. *Quat. Sci. Rev.* **21**, 295–305 (2002).
7. Takagi, H. et al. Characterizing photosymbiosis in modern planktonic foraminifera. *Biogeosciences* **16**, 3377–3396 (2019).
8. Gradstein, F. M. Evolution and Biostratigraphy. in *Geologic Time Scale 2020* 35–137 (Elsevier, 2020). https://doi.org/10.1016/B978-0-12-824360-2.00003-6.
9. Hohenegger, J. Foraminiferal growth and test development. *Earth. Sci. Rev.* **185**, 140–162 (2018).
10. de Nooijer, L. J., Spero, H. J., Erez, J., Bijma, J. & Reichart, G. J. Biomineralization in perforate foraminifera. *Earth. Sci. Rev.* **135**, 48–58 (2014).
11. Spero, H. J., Bijma, J., Lea, D. W. & Bemis, B. E. Spero et al. 1997_N. 497–500 (1997).
12. Erez, J. *The Source of Ions for Biomineralization in Foraminifera and Their Implications for Paleoceanographic Proxies*. http://pubs.geoscienceworld.org/msa/rimg/article-pdf/54/1/115/2944286/115.gsrmg.54.pdf.
13. Rathmann, S. & Kuhnert, H. Carbonate ion effect on Mg/Ca, Sr/Ca and stable isotopes on the benthic foraminifera Oridorsalis umbonatus off Namibia. *Mar. Micropaleontol.* **66**, 120–133 (2008).
14. Rollion-Bard, C., Erez, J. & Zilberman, T. Intra-shell oxygen isotope ratios in the benthic foraminifera genus Amphistegina and the

influence of seawater carbonate chemistry and temperature on this ratio. *Geochim. Cosmochim. Acta* **72**, 6006–6014 (2008).
15. Spero, H. J. *Do Planktic Foraminifera Accurately Record Shifts in the Carbon Isotopic Composition of Seawater ZC02? Marine Micropaleontology* vol. 19 (1992).
16. Spero, H. J. & Lea, D. W. *Intraspecific Stable Isotope Variability in the Planktic Foraminifera Globigerinoides Sacculifer: Results from Laboratory Experiments*. *Marine Micropaleontology* vol. 22 (1993).
17. Bemis, B. E., Spero, H. J., Bijma, J. & Lea, D. W. Reevaluation of the oxygen isotopic composition of planktonic foraminifera: Experimental results and revised paleotemperature equations. *Paleoceanography* **13**, 150–160 (1998).
18. Lynch-Stieglitz, J., Curry, W. & Paleoceanography, N. S. A geostrophic transport estimate for the Florida Current from the oxygen isotope composition of *benthic foraminifera*. *Wiley Online Libr.* **14**, 360–373 (1999).
19. Spero, H. J. & Lea, D. W. Experimental determination of stable isotope variability in Globigerina bulloides: implications for paleoceanographic reconstructions. *Mar. Micropaleontol.* **28**, 231–246 (1996).
20. Marchitto, T. M. et al. Improved oxygen isotope temperature calibrations for cosmopolitan benthic foraminifera. *Geochim. Cosmochim. Acta* **130**, 1–11 (2014).
21. Mulitza, S. et al. Temperature:δ18O relationships of planktonic foraminifera collected from surface waters. *Palaeogeogr. Palaeoclimatol. Palaeoecol.* **202**, 143–152 (2003).
22. Keigwin, L. D. Glacial-age hydrography of the far northwest Pacific Ocean. *Paleoceanography* **13**, 323–339 (1998).
23. Meckler, A. N. et al. Cenozoic evolution of deep ocean temperature from clumped isotope thermometry. *Science* **377**, 86–90 (2022).
24. Kocken, I. J. et al. North Atlantic temperature change across the Eocene-Oligocene transition from clumped isotopes. *Paleoceanogr. Paleoclimatol*. **39**, (2024).
25. Agterhuis, T., Ziegler, M., de Winter, N. J. & Lourens, L. J. Warm deep-sea temperatures across Eocene Thermal Maximum 2 from clumped isotope thermometry. *Commun. Earth Environ.* **3**, 39 (2022).
26. Meinicke, N., Reimi, M. A., Ravelo, A. C. & Meckler, A. N. Coupled Mg/Ca and clumped isotope measurements indicate lack of substantial mixed layer cooling in the western Pacific warm pool during the last ~5 million years. *Paleoceanogr. Paleoclimatol*. **36**, (2021).
27. Modestou, S. E., Leutert, T. J., Fernandez, A., Lear, C. H. & Meckler, A. N. Warm middle miocene indian ocean bottom water temperatures: comparison of clumped isotope and Mg/Ca-based estimates. *Paleoceanogr. Paleoclimatol*. **35**, (2020).
28. Evans, D. et al. Eocene greenhouse climate revealed by coupled clumped isotope-Mg/Ca thermometry. *Proc. Natl. Acad. Sci. USA* **115**, 1174–1179 (2018).
29. Peral, M. et al. Changes in temperature and oxygen isotopic composition of Mediterranean water during the Mid-Pleistocene transition in the Montalbano Jonico section (southern Italy) using the clumped-isotope thermometer. *Palaeogeogr. Palaeoclimatol. Palaeoecol.* **544**, 109603 (2020).
30. Schauble, E. A., Ghosh, P. & Eiler, J. M. Preferential formation of 13C-18O bonds in carbonate minerals, estimated using first-principles lattice dynamics. *Geochim. Cosmochim. Acta* **70**, 2510–2529 (2006).
31. Grauel, A. L. et al. Calibration and application of the 'clumped isotope' thermometer to foraminifera for high-resolution climate reconstructions. *Geochim. Cosmochim. Acta* **108**, 125–140 (2013).
32. Tripati, A. K. et al. 13C-18O isotope signatures and 'clumped isotope' thermometry in foraminifera and coccoliths. *Geochim. Cosmochim. Acta* **74**, 5697–5717 (2010).
33. Tripati, A. K. et al. Modern and glacial tropical snowlines controlled by sea surface temperature and atmospheric mixing. *Nat. Geosci.* **7**, 205–209 (2014).
34. Müller, I. A. et al. Carbonate clumped isotope analyses with the long-integration dual-inlet (LIDI) workflow: scratching at the lower sample weight boundaries. *Rapid Commun. Mass Spectrom.* **31**, 1057–1066 (2017).
35. Peral, M. et al. Updated calibration of the clumped isotope thermometer in planktonic and benthic foraminifera. *Geochim. Cosmochim. Acta* **239**, 1–16 (2018).
36. Bernasconi, S. M. et al. Reducing uncertainties in carbonate clumped isotope analysis through consistent carbonate-based standardization. *Geochem. Geophys. Geosyst.* **19**, 2895–2914 (2018).
37. Meckler, A. N., Ziegler, M., Millán, M. I., Breitenbach, S. F. M. & Bernasconi, S. M. Long-term performance of the Kiel carbonate device with a new correction scheme for clumped isotope measurements. *Rapid Commun. Mass Spectrom.* **28**, 1705–1715 (2014).
38. Hu, B. et al. A modified procedure for gas-source isotope ratio mass spectrometry: the long-integration dual-inlet (LIDI) methodology and implications for clumped isotope measurements. *Rapid Commun. Mass Spectrom.* **28**, 1413–1425 (2014).
39. Meinicke, N. et al. A robust calibration of the clumped isotopes to temperature relationship for foraminifers. *Geochim. Cosmochim. Acta* **270**, 160–183 (2020).
40. Breitenbach, S. F. M. et al. Coupled Mg/Ca and clumped isotope analyses of foraminifera provide consistent water temperatures. *Geochim. Cosmochim. Acta* **236**, 283–296 (2018).
41. Bernasconi, S. M. et al. InterCarb: a community effort to improve interlaboratory standardization of the carbonate clumped isotope thermometer using carbonate standards. *Geochem. Geophys. Geosyst.* **22**, 1–25 (2021).
42. Anderson, N. T. et al. A unified clumped isotope thermometer calibration (0.5–1,100 °C) using carbonate-based standardization. *Geophys. Res. Lett.* **48**, 1–11 (2021).
43. Daëron, M. & Vermeesch, P. Omnivariant generalized least squares regression: theory, geochronological applications, and making the case for reconciled Δ47 calibrations. *Chem. Geol.* **647**, 121881 (2024).
44. Peral, M. et al. On the combination of the planktonic foraminiferal Mg/Ca, clumped (Δ47) and conventional (δ18O) stable isotope paleothermometers in palaeoceanographic studies. *Geochim. Cosmochim. Acta* **339**, 22–34 (2022).
45. Daëron, M. & Gray, W. R. Revisiting oxygen-18 and clumped isotopes in planktic and *Benthic Foraminifera*. *Paleoceanogr. Paleoclimatol*. **38**, (2023).
46. Piasecki, A. et al. Application of clumped isotope thermometry to Benthic Foraminifera. *Geochem. Geophys. Geosyst.* **20**, 2082–2090 (2019).
47. Schiebel, R. & Hemleben, C. *Planktic Foraminifers in the Modern Ocean*. (2017).
48. Zaarur, S., Affek, H. P. & Brandon, M. T. A revised calibration of the clumped isotope thermometer. *Earth Planet. Sci. Lett.* **382**, 47–57 (2013).
49. Huber, M. A hotter greenhouse? *Science* **321**, 353–354 (2008).
50. Huber, M. & Sloan, L. C. Climatic responses to tropical sea surface temperature changes on a "greenhouse" Earth. *Paleoceanography* **15**, 443–450 (2000).
51. Pearson, P. N. et al. Warm tropical sea surface temperatures in the Late Cretaceous and Eocene epochs. *Nature* **413**, (2001).
52. Fiebig, J. et al. Combined high-precision Δ48 and Δ47 analysis of carbonates. *Chem. Geol.* **522**, 186–191 (2019).
53. Fiebig, J. et al. Calibration of the dual clumped isotope thermometer for carbonates. *Geochim. Cosmochim. Acta* **312**, 235–256 (2021).

54. Bernecker, M. et al. A robust methodology for triple (Δ47, Δ48, Δ49) clumped isotope analysis of carbonates. *Chem. Geol*. **642**, (2023).
55. Fiebig, J. et al. Carbonate clumped isotope values compromised by nitrate-derived NO2 interferent. *Chem. Geol*. **670**, (2024).
56. Hill, P. S., Tripati, A. K. & Schauble, E. A. Theoretical constraints on the effects of pH, salinity, and temperature on clumped isotope signatures of dissolved inorganic carbon species and precipitating carbonate minerals. *Geochim. Cosmochim. Acta* **125**, 610–652 (2014).
57. Daëron, M. et al. Most Earth-surface calcites precipitate out of isotopic equilibrium. *Nat. Commun.* **10**, 1–7 (2019).
58. Daëron, M. Full propagation of analytical uncertainties in Δ47 measurements. *Geochem. Geophys. Geosyst.* **22**, 1–19 (2021).
59. Locarnini, R. A. et al. World Ocean Atlas 2018, Volume 1*: Temperature*. vol. 1 http://www.nodc.noaa.gov/OC5/indprod.html (2018).
60. Davies, A. J. et al. Isotopic disequilibrium in brachiopods disentangled with dual clumped isotope thermometry. *Geochim. Cosmochim. Acta* **359**, 135–147 (2023).
61. Clark, A. J., Jaggi, M., Bernasconi, S. M., Fiebig, J. & Stoll, H. M. Clumped isotope temperatures of coccolithophores from global sediment traps. *Paleoceanogr. Paleoclimatol*. **40**, (2025).
62. Coplen, T. B. Calibration of the calcite-water oxygen-isotope geothermometer at Devils Hole, Nevada, a natural laboratory. *Geochim. Cosmochim. Acta* **71**, 3948–3957 (2007).
63. Bajnai, D. et al. Devils hole calcite was precipitated at ±1 °C stable aquifer temperatures during the last half million years. *Geophys. Res. Lett*. **48**, (2021).
64. Kim, S. T. & O'Neil, J. R. Equilibrium and nonequilibrium oxygen isotope effects in synthetic carbonates. *Geochim. Cosmochim. Acta* **61**, 3461–3475 (1997).
65. Shackleton, N. J. Attainment of isotopic equilibrium between ocean water and the benthonic foraminifera genus Uvigerina: isotopic changes in the ocean during the last glacial. *Colloq. Int. du C. N. R. S* **219**, 203 (1974).
66. Davies, A. J. et al. Dual clumped isotope thermometry of coral carbonate. *Geochim. Cosmochim. Acta* **338**, 66–78 (2022).
67. Bentov, S. & Erez, J. Novel observations on biomineralization processes in foraminifera and implications for Mg/Ca ratio in the shells. *Geology* 841–844 (2005) https://doi.org/10.1130/G21800.1.
68. Bentov, S., Brownlee, C. & Erez, J. The role of seawater endocytosis in the biomineralization process in calcareous foraminifera. *Proc. Natl. Acad. Sci. USA* **106**, 21500 (2009).
69. de Nooijer, L. J., Toyofuku, T. & Kitazato, H. Foraminifera promote calcification by elevating their intracellular pH. *Proc. Natl. Acad. Sci. USA* **106**, 15374–15378 (2009).
70. Toyofuku, T. et al. Proton pumping accompanies calcification in foraminifera. *Nat. Commun.* **8**, 1–6 (2017).
71. Schulz, K. G., Riebesell, U., Rost, B., Thoms, S. & Zeebe, R. E. Determination of the rate constants for the carbon dioxide to bicarbonate inter-conversion in pH-buffered seawater systems. *Mar. Chem.* **100**, 53–65 (2006).
72. Hauzer, H., Evans, D., Müller, W., Rosenthal, Y. & Erez, J. The effect of carbonate chemistry on trace element incorporation in high-Mg calcitic foraminifera. *Geochim. Cosmochim. Acta* **390**, 105–116 (2025).
73. Dubicka, Z., Bojanowski, M. J., Bijma, J. & Bickmeyer, U. Mg-rich amorphous to Mg-low crystalline CaCO3 pathway in foraminifera. *Heliyon* **9**, e18331 (2023).
74. Jacob, D. E., Wirth, R., Agbaje, O. B. A., Branson, O. & Eggins, S. M. Planktic foraminifera form their shells via metastable carbonate phases. https://doi.org/10.1038/s41467-017-00955-0.
75. Arns, A. I. et al. Mesocrystalline architecture in hyaline foraminifer shells indicates a non-classical crystallisation pathway. *Geochem. Geophys. Geosyst.* **23**, e2022GC010445 (2022).
76. Guo, W. Kinetic clumped isotope fractionation in the DIC-H2O-CO2 system: patterns, controls, and implications. *Geochim. Cosmochim. Acta* **268**, 230–257 (2020).
77. François, D., Reichart, G.-J. & de Nooijer, L. J. Open or closed: pH modulation and calcification by foraminifera. *Sci. Adv.* **11**, 8425 (2025).
78. Rink, S., Kühl, M., Bijma, J. & Spero, H. J. Microsensor studies of photosynthesis and respiration in the symbiotic foraminifer Orbulina universa. *Mar. Biol.* **131**, 583–595 (1998).
79. Rollion-Bard, C. & Blamart, D. Possible controls on Li, Na, and Mg incorporation into aragonite coral skeletons. *Chem. Geol.* **396**, 98–111 (2015).
80. Evans, D., Brugger, J., Inglis, G. N. & Valdes, P. The temperature of the deep ocean is a robust proxy for global mean surface temperature during the Cenozoic. *Paleoceanogr. Paleoclimatol.* **39**, e2023PA004788 (2024).
81. Zeebe, R. E. History of seawater carbonate chemistry, atmospheric CO_2, and ocean acidification. *Annu. Rev. Earth Planet. Sci.* **40**, 141–165 (2012).
82. Bice, K. L. et al. A multiple proxy and model study of Cretaceous upper ocean temperatures and atmospheric CO2 concentrations. *Paleoceanography* **21**, (2006).
83. Royer, D. L., Berner, R. A., Montanez, I. P., Tabor, N. J. & Beerling, D. J. CO2 as a primary driver of Phanerozoic climate. *GSA Today* **14**, 4–10 (2004).
84. Uchikawa, J. & Zeebe, R. E. Examining possible effects of seawater pH decline on foraminiferal stable isotopes during the Paleocene-Eocene Thermal Maximum. *Paleoceanography* **25**, (2010).
85. Beck, W. C., Grossman, E. L. & Morse, J. W. Experimental studies of oxygen isotope fractionation in the carbonic acid system at 15°, 25°, and 40 °C. *Geochim. Cosmochim. Acta* **69**, 3493–3503 (2005).
86. Usdowski, E. & Hoefs, J. Oxygen isotope exchange between carbonic acid, bicarbonate, carbonate, and water: A re-examination of the data of McCrea (1950) and an expression for the overall partitioning of oxygen isotopes between the carbonate species and water. *Geochim. Cosmochim. Acta* **57**, 3815–3818 (1993).
87. Zeebe, R. E. An explanation of the effect of seawater carbonate concentration on foraminiferal oxygen isotopes. *Geochim. Cosmochim. Acta* **63**, 2001–2007 (1999).
88. Watkins, J. M. & Hunt, J. D. A process-based model for non-equilibrium clumped isotope effects in carbonates. *Earth Planet. Sci. Lett.* **432**, 152–165 (2015).
89. Watkins, J. M. & Devriendt, L. S. A combined model for kinetic clumped isotope effects in the CaCO3-DIC-H2O system. *Geochem. Geophys. Geosyst.* **23**, (2022).
90. Huyghe, D., Lartaud, F., Emmanuel, L., Merle, D. & Renard, M. Palaeogene climate evolution in the Paris Basin from oxygen stable isotope (δ18O) compositions of marine molluscs. *J. Geol. Soc. Lond.* **172**, 576–587 (2015).
91. Kniest, J. F. et al. Dual clumped isotopes from Mid-Eocene bivalve shell reveal a hot and summer wet climate of the Paris Basin. *Commun. Earth Environ.* **5**, 1–10 (2024).
92. King, C. *A Revised Correlation of Tertiary Rocks in the British Isles and Adjacent Areas of NW Europe*. (The Geological Society of London, 2016). https://doi.org/10.1144/SR27.
93. Schlidt, V. et al. Most bivalves and gastropods calcify indistinguishably from dual clumped isotope equilibrium. *Geochim. Cosmochim. Acta* **410**, 174–187 (2025).
94. Swart, P. K. et al. A calibration equation between Δ48 values of carbonate and temperature. *Rapid Commun. Mass Spectrometry* **35**, (2021).
95. Caley, T. et al. High-latitude obliquity as a dominant forcing in the Agulhas current system. *Climate* **7**, 1285–1296 (2011).
96. Peral, M. et al. Understanding the relationship between foraminiferal Mg/Ca and clumped isotope thermometers. *Geochim. Cosmochim. Acta* **407**, 253–264 (2025).

97. Bahr, A. et al. South American Hydrological Balance and Paleoceanography during the Late Pleistocene and Holocene (SAMBA)–Cruise No. M125, March 21–April 15, 2016–Rio de Janeiro (Brazil)–Fortaleza (Brazil). https://doi.org/10.2312/cr_m125 (2016)
98. Renema, W., Beaman, R. J. & Webster, J. M. Mixing of relict and modern tests of larger benthic foraminifera on the Great Barrier Reef shelf margin. *Mar. Micropaleontol.* **101**, 68–75 (2013).
99. Locarnini, R. A. et al. World Ocean Atlas 2013. Vol. 1: Temperature. *S*. Levitus, *Ed.;* A. Mishonov, Technical *Ed.; NOAA Atlas NESDIS* **73**, 40 (2013).
100. Oron, S., Evans, D., Abramovich, S., Almogi-Labin, A. & Erez, J. Differential sensitivity of a symbiont-bearing Foraminifer to seawater carbonate chemistry in a decoupled DIC-pH experiment. *J. Geophys. Res. Biogeosci.* **125**, e2020JG005726 (2020).
101. Roche, D. M., Waelbroeck, C., Metcalfe, B. & Caley, T. FAME (v1.0): A simple module to simulate the effect of planktonic foraminifer species-specific habitat on their oxygen isotopic content. *Geosci. Model Dev.* **11**, 3587–3603 (2018).
102. Curry, D. et al. The Bracklesham Beds (Eocene) of Bracklesham Bay and Selsey, Sussex. *PrGA* **88**, 243–254 (1977).
103. Gale, A. *The Isle of Wight* [*Geologists' Association Guide*]. (Geologists' Association, 2019).
104. Nolf, D., Steurbaut, É & Cahuzac, B. Progrès récents dans la connaissance des gisements cénozoïques en aquitaine méridionale (Chalosse, Béarn et Bas-Adour; SW France). *Rev. de. Micropaléontologie* **45**, 169–194 (2002).
105. Nambiar, R. Long-term variability of ocean chemistry: implications for deep-time palaeothermometry and the carbon cycle. *Doctoral dissertation, Universitätsbibliothek Johann Christian Senckenberg* (2024).
106. Lombard, F., Labeyrie, L., Michel, E., Spero, H. J. & Lea, D. W. Modelling the temperature dependent growth rates of planktic foraminifera. *Mar. Micropaleontol.* **70**, 1–7 (2009).
107. LeGrande, A. N. & Schmidt, G. A. Global gridded data set of the oxygen isotopic composition in seawater. *Geophys. Res. Lett.* **33**, 1–5 (2006).
108. Kim, S. T., Mucci, A. & Taylor, B. E. Phosphoric acid fractionation factors for calcite and aragonite between 25 and 75 °C: revisited. *Chem. Geol.* **246**, 135–146 (2007).
109. Dennis, K. J., Affek, H. P., Passey, B. H., Schrag, D. P. & Eiler, J. M. Defining an absolute reference frame for 'clumped' isotope studies of CO2. *Geochim. Cosmochim. Acta* **75**, 7117–7131 (2011).
110. Petersen, S. V. et al. Effects of improved 17 O correction on interlaboratory agreement in clumped isotope calibrations, estimates of mineral-specific offsets, and temperature dependence of acid digestion fractionation. *Geochem. Geophys. Geosyst.* **20**, 3495–3519 (2019).
111. Bernecker, M., Daëron, M., Staudigel, P. T., Hofmann, S. & Fiebig, J. D.4Xgui: A tool for baseline correction and standardization of carbonate clumped isotope raw data. *SoftwareX* **33**, (2026).
112. APA, A. P. Publications manual of the American Psychological Association: the official guide to APA style (ed.). (American Psychological Association, 2020).
113. Davies, A. J. et al. Supplementary Files to 'Dual clumped isotopes in foraminiferal calcite reveal kinetic bias in some species'. *Zenodo* https://doi.org/10.5281/zenodo.20594013.

Acknowledgements

The authors would like to thank Sven Hofmann, Niels Meijier, Armelle Ballian and Manuel Schuman for assistance in the laboratory. No permission was required for sampling of LBF from the Hampshire and Paris Basins. This research was funded through the VeWA consortium by the LOEWE programme of the Hessen Ministry of Higher Education, Research and the Arts, Germany, and through FI-948-13/1 granted to JF. The ARTEMIS radiocarbon dating project is acknowledged.

Author contributions

Initial design was conceived by A.J.D. and J.F. A.D., J.F., M.T., P.T. and M.B. were responsible for clumped and stable isotope data acquisition and processing. M.P., T.C., O.F. and D.E. provided samples of recent foraminifera. D.C., R.N. and D.E. provided Eocene foraminifera. J.E. and A.L. cultured large benthic foraminifera. T.C. ran the FAME model and carried out core-top dating for site MD96-2048. P.S. ran the growth rate model for isotopic disequilibrium. J.F. was responsible for funding acquisition. A.J.D. wrote the first draft of the manuscript. All authors contributed to the writing process.

Funding

Open Access funding enabled and organized by Projekt DEAL.

Competing interests

The authors declare no competing interests.

Additional information

Supplementary information The online version contains supplementary material available at https://doi.org/10.1038/s43247-026-03770-y.

Correspondence and requests for materials should be addressed to Amelia Jane Davies or Jens Fiebig.

Peer review information *Communications Earth & Environment* thanks Nele Meckler, Mathieu Daëron and the other, anonymous, reviewer(s) for their contribution to the peer review of this work. Primary Handling Editors: Yiming Wang and Somaparna Ghosh. A peer review file is available.